Zeitschrift: IABSE congress report = Rapport du congrès AIPC = IVBH Kongressbericht

Band: 4 (1952)

Artikel: The calculation of plastic collapse loads for plane frames

Autor: Neal, B.G. / Symonds, P.S.

DOI: https://doi.org/10.5169/seals-5020

AI 3

The calculation of plastic collapse loads for plane frames

Le calcul des charges plastiques de rupture des cadres plans

Die Berechnung der plastischen Brucklasten ebener Rahmentragwerke

B. G. NEAL and P. S. SYMONDS

Engineering Department, Cambridge University

Brown University, Providence, R.I., U.S.A.

INTRODUCTION

Plastic design methods have been developed with a view to providing a more rational and economical approach to the design of framed structures whose members possess a high degree of ductility.[1] The methods are applicable to cases in which the members of a frame possess a relation between bending moment and curvature of the form illustrated in fig. 1. The important features of this type of relation are:

(i) If the curvature increases indefinitely, the bending moment tends to a limiting value $\pm M_p$, termed the fully plastic moment, regardless of the previous history of loading.

(ii) An increase of curvature is always accompanied by an increase of bending moment of the same sign, unless the bending moment has attained its fully plastic value.

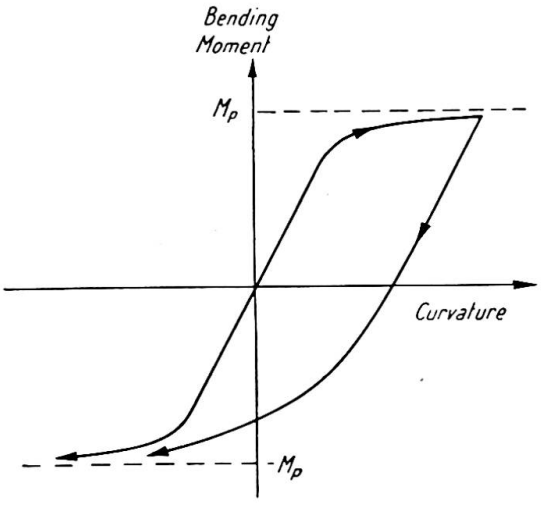

Fig. 1

The behaviour of mild steel beams conforms quite closely to these assumptions, and experimental investigations have confirmed the validity of applying plastic methods of design to framed structures of mild steel.[2] As yet, little consideration has been given to the possibility of applying the plastic methods

[1] For references see end of paper.

to framed structures of other ductile materials, such as certain of the light alloys.

When the fully plastic moment is attained at a particular cross-section of a member, the curvature at this cross-section is indefinitely large, so that a finite change of slope can occur over an indefinitely short length of the member at this cross-section. The member therefore behaves as though a hinge existed at this cross-section, rotation of the hinge being possible only when resisted by the fully plastic moment. This concept of a plastic hinge was first introduced by Maier-Leibnitz,[3] and it is of great value in considering the behaviour of framed structures under load.

For the sake of simplicity, consider first a framed structure subjected to several loads, each load maintaining the same proportion to each of the other loads. If the loads are steadily increased, the structure will first support the loads by wholly elastic action. Eventually a plastic hinge will form at the most highly stressed cross-section. If the loads are increased still further, this plastic hinge will rotate under a constant bending moment, its fully plastic moment, and further plastic hinges will form and rotate in other parts of the structure. Finally, a condition will be reached in which a sufficient number of plastic hinges have formed to transform the structure into a mechanism. The structure will then continue to deform to an indefinite extent while the loads remain constant, until the geometry of the structure is changed appreciably. Such changes may either check the growth of the deflections, or cause a catastrophic collapse by accentuating the effects of the loads. In practice, strain-hardening also checks the growth of deflections. The theoretical condition of indefinite growth of deflection under constant loads is termed plastic collapse.

The methods of plastic design are used in conjunction with a load factor. The structure is designed so that the most unfavourable combination of the working loads, when multiplied by the chosen load factor, would just cause a failure by plastic collapse. This procedure is justifiable even when the loads do not necessarily maintain the same proportions to one another, for it has been shown that plastic collapse of a structure will occur at the same set of loads regardless of the sequence in which the individual loads were brought up to their collapse values. It is clear that the load factor has a very precise meaning in plastic design, for it represents the margin of safety which is provided against an actual physical failure of the structure.

Several methods for computing plastic collapse loads have been suggested.[4, 5] These methods have been capable, in principle, of determining plastic collapse loads for framed structures of any degree of complexity. In practice, however, their application has been limited by the amount of time required for the necessary computations. In the present paper a method is presented which enables plastic collapse loads and their corresponding mechanisms to be determined very simply. The method consists essentially of building up the actual collapse mechanism from a certain number of independent components, which are termed the independent partial collapse mechanisms. Corresponding to any mechanism which is being investigated, a value can be found for the applied load by applying the Principle of Virtual Work.[6] It has been shown that the correct collapse mechanism is the one to which there corresponds the smallest possible value of the applied load. The method consists therefore of combining the independent partial collapse mechanisms in a systematic manner in order to reduce the corresponding value of the applied load to its least possible value. In order to explain and justify the method, a simple example will first be discussed. Detailed calculations will then be given for a single-bay pitched-roof portal frame, and the calculations for a three-bay pitched-roof portal frame will also be outlined. Calculations for a two-bay three-storey rectangular frame have been given elsewhere.[7]

SIMPLE ILLUSTRATIVE EXAMPLE

The rectangular portal frame shown in fig. 2 will be used as a basis for the discussion of the method. All the joints of this frame are assumed to be rigid, and the feet of the stanchions are rigidly built in. The dimensions of the frame are as shown, and horizontal and vertical loads W are applied at the positions indicated in the figure. The fully plastic moment of each member is M_p, and the problem is to find the value of W which causes failure by plastic collapse.

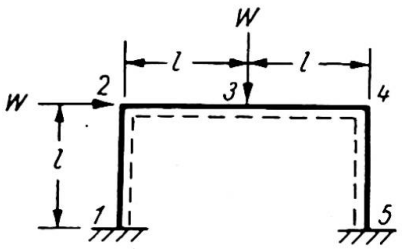

Fig. 2

For this particular type of structure it is known that there are only three possible collapse mechanisms, and these mechanisms are shown in figs. 3(*a*), 3 (*b*) and 3(*c*). In these figures the magnitudes of the plastic hinge rotations are all shown in terms of a single parameter θ. For reference, the signs of the plastic hinge rotations are also given, although in the technique to be described there is no need to take account of these signs. The sign convention adopted is that a hinge rotation is positive if the hinge is opening when viewed from inside the frame.

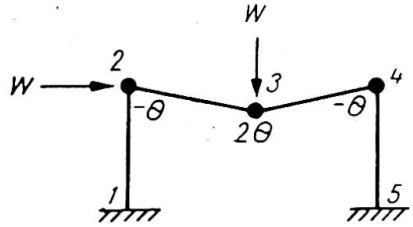

Fig. 3(*a*)

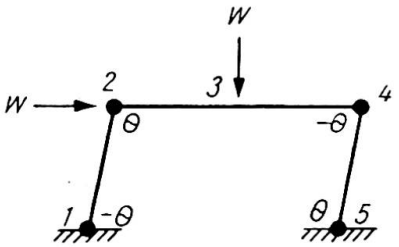

Fig. 3(*b*)

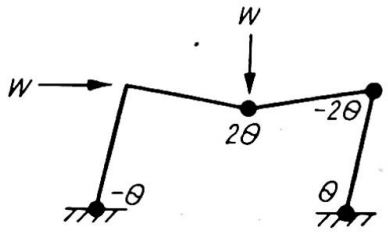

Fig. 3(*c*)

For each mechanism it is possible to calculate a corresponding value of W by applying the principle of virtual work in the special form that the virtual work done by the applied loads during a small displacement of the mechanism is equal to the virtual work absorbed in the plastic hinges. Considering the mechanism of fig. 3(*a*), for example, it is seen that during the small mechanism displacement shown, the horizontal load W does no work and the vertical load W, displaced through a distance $l\theta$, does virtual work $Wl\theta$. To calculate the virtual work absorbed in the plastic hinges, it is noted that the work absorbed in any individual hinge is always positive. Since the fully plastic moment is M_p everywhere in the frame, the virtual work absorbed in the plastic hinges is at once seen to be $4\theta M_p$, since the total rotation of all the plastic hinges is 4θ. Applying the principle of virtual work:

$$Wl\theta = 4\theta M_p, \text{ or } W = 4\frac{M_p}{l} \quad . \quad . \quad . \quad . \quad . \quad . \quad . \quad . \quad (1)$$

Similar calculations for the mechanisms of figs. 3(*b*) and 3(*c*) are readily made. The results of these calculations are:

fig. 3(*b*): $$Wl\theta=4\theta M_p, \text{ or } W=4\frac{M_p}{l} \quad . \ . \ . \ . \ . \ . \ . \ . \quad (2)$$

fig. 3(*c*): $$2Wl\theta=6\theta M_p, \text{ or } W=3\frac{M_p}{l} \quad . \ . \ . \ . \ . \ . \ . \ . \quad (3)$$

The correct collapse mechanism can now be distinguished by applying what has been termed the *kinematic principle* of plastic collapse.[6, 8] This principle states that: " For a given frame and loading, the correct collapse mechanism is the mechanism to which there corresponds the smallest possible value of the applied loads." For the particular problem of fig. 2, it follows that the actual collapse mechanism is the mechanism shown in fig. 3(*c*), which yields the lowest value of W, namely $3M_p/l$.

Examination of figs. 3(*a*), 3(*b*) and 3(*c*) reveals the fact that the mechanism of fig. 3(*c*) is a direct combination of the mechanisms of figs. 3(*a*) and 3(*b*), in the sense that the displacements and plastic hinge rotations of this mechanism are obtained by summing the corresponding quantities for the mechanisms of figs. 3(*a*) and 3(*b*). In fact, as will be seen later, these latter two mechanisms are the independent partial collapse mechanisms for this structure and loading. In general, all possible collapse mechanisms can be formed by combining the independent partial collapse mechanisms. In the simple problem under consideration there is, of course, only one possible combination to be investigated.

The particular feature of the combination of the independent mechanisms of figs. 3(*a*) and 3(*b*) which is of interest is that for both these mechanisms the corresponding value of W was $4M_p/l$, whereas for the mechanism of fig. 3(*c*) which resulted from their combination the value of W was only $3M_p/l$. This reduction of W is due to the cancellation of the plastic hinge at the cross-section 2 which occurs when the mechanisms are combined. When the two mechanisms are superposed, the virtual work done by the loads in each case may be added to obtain the virtual work done in the resulting mechanism. However, to obtain the virtual work absorbed in the plastic hinges in the resulting mechanism, work $2\theta M_p$ must be subtracted from the sum of the virtual work absorbed in the two independent mechanisms. This is to account for the term θM_p which was included in the virtual work absorbed in each of these mechanisms for the plastic hinge at the cross-section 2, which disappears as a result of the superposition. The virtual work equation for the resulting mechanism is thus obtained by adding equations (1) and (2), and subtracting $2\theta M_p$ from the resulting work absorbed in the plastic hinges, giving:

$$Wl\theta+Wl\theta=4\theta M_p+4\theta M_p-2\theta M_p$$

or $$2Wl\theta=6\theta M_p,$$

which was previously obtained as equation (3).

In general, the technique for combining the independent mechanisms thus consists in selecting pairs of independent mechanisms which themselves yield low values of W, and which can be combined so as to cancel a plastic hinge. Such a combination may, as has been seen, result in a value for W which is lower than the value corresponding to either of the mechanisms which were combined. Even in complicated problems, the combinations to be tried are usually small in number, so that a solution can be obtained with great rapidity.

It is, of course, essential to start an analysis with the correct number of independent mechanisms. In fact, the number of independent mechanisms is always equal to the

number of independent equations of equilibrium for the frame. To justify this statement, it is necessary to consider the statics of the illustrative example of fig. 2, although it should be stressed that in actual applications of the technique there is no need to write down the equations of equilibrium. However, it is recommended that solutions should always be checked by statics, making use of the *principle of uniqueness of solution*,[6, 8] which states that: "If a sufficient number of plastic hinges occur in a frame to transform the frame into a mechanism, and if a bending moment diagram can be constructed for the frame in which the fully plastic moment occurs at each plastic hinge position, then the corresponding load is the correct collapse load if the fully plastic moment is not exceeded anywhere in the frame."

Examples of this form of check are given later in the paper.

The equations of equilibrium

The equations of equilibrium for the frame illustrated in fig. 2 are written down most conveniently in terms of the bending moments at the five cross-sections numbered from 1 to 5 in fig. 2. It will be seen from this figure that when these five bending moments are known, the bending moment distribution for the entire frame is determined, for between any adjacent pair of these cross-sections the shear force is constant, so that the bending moment must vary linearly along the length of the member. These five bending moments are denoted by $M_1, M_2, \ldots M_5$, the suffix indicating the relevant cross-section. The sign convention adopted for these bending moments is that a positive bending moment causes tension in the fibres of a member adjacent to the dotted line in fig. 2.

This frame has three redundancies, for if a cut is imagined to be made at section 1, for example, and the values of the shear force, thrust and bending moment at this section are known, the entire frame becomes statically determinate. These three quantities can therefore be regarded as the redundancies of the frame. Since there are five unknown bending moments, it follows that there must be two independent equations of equilibrium.

The first of these equations of equilibrium expresses the fact that the vertical load W is carried by the shear forces in the horizontal member 234. Fig. 4 shows the

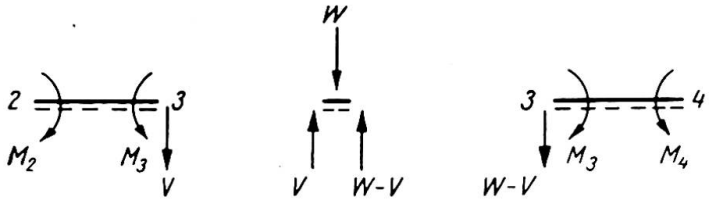

Fig. 4

relevant forces and bending moments, the load W being carried by a shear force V in the member 23 and a shear force $W-V$ in the member 34. Taking moments for the equilibrium of the members 23 and 34, it is found that

$$M_3-M_2=Vl$$

$$M_3-M_4=(W-V)l$$

On adding these equations to eliminate V, it is found that

$$2M_3-M_2-M_4=Wl \quad . \quad . \quad . \quad . \quad . \quad . \quad . \quad . \quad (4)$$

In a similar way, an equation expressing the fact that the horizontal load W is carried

by the shear forces in the vertical members 12 and 45 may be found. This equation is

$$M_2-M_1+M_5-M_4=Wl \quad . \quad . \quad . \quad . \quad . \quad . \quad . \quad . \quad (5)$$

Equations (4) and (5) constitute the two independent equations of equilibrium.

In the mechanism of fig. 3(*a*) plastic hinges have formed at the cross-sections 2, 3 and 4, so that the magnitude of the bending moment at each of these cross-sections is M_p. Having regard to the sign convention, these bending moments are

$$M_2=-M_p, \quad M_3=M_p, \quad M_4=-M_p$$

When these values are substituted in equation (4), a value for W is immediately found, this value being $W=4M_p/l$.

It will be seen that the mechanism of fig. 3(*a*) corresponds to equation (4) in the special sense that in this mechanism each of the bending moments appearing in equation (4) takes on its fully plastic value, and that the sign of each bending moment is such as to give rise to the largest possible value of W. In a similar way, the mechanism of fig. 3(b) may be said to correspond to equation (5). If each of the bending moments appearing in equation (5) is given its fully plastic value, and the sign of each bending moment is such that the largest value of W is obtained, the following values are found:

$$M_1=-M_p, \quad M_2=M_p, \quad M_4=-M_p, \quad M_5=M_p.$$

These are the fully plastic moments appearing in the mechanism of fig. 3(*b*).

To generalise, it may be said that any mechanism corresponds in this special sense to a particular equation of equilibrium. It follows that for any particular frame and loading the number of independent mechanisms will be equal to the number of independent equations of equilibrium. In the particular example under consideration there are only two independent equations of equilibrium, namely equations (4) and (5) and any other equation of equilibrium must be obtainable by combining these two equations. Correspondingly, it follows that any possible mechanism will be found to be a combination of the mechanisms of figs. 3(*a*) and 3(*b*). In this particular example, there is only one possible combination of these mechanisms, which is illustrated in fig. 3(*c*). The equation of equilibrium which corresponds to this mechanism is obtained by adding equations (4) and (5) so as to eliminate M_2, giving

$$2M_3-M_1-2M_4+M_5=2Wl \quad . \quad . \quad . \quad . \quad . \quad . \quad . \quad (6)$$

This addition corresponds to the superposition of the mechanisms of figs. 3(*a*) and 3(*b*). The bending moments at the plastic hinges may be seen from this equation, or from the mechanism of fig. 3(*c*), to be

$$M_1=-M_p, \quad M_3=M_p, \quad M_4=-M_p, \quad M_5=M_p,$$

and the corresponding value of W is $3M_p/l$.

For convenience of discussion, the loads have previously been referred to as the variables, whereas in an actual design the loads will be given quantities and the problem is to find the required fully plastic moments of the members. When viewed in this light, the problem just discussed amounts to determining the *greatest* value of M_p, rather than the least value of W, corresponding to any possible mechanism, for it is the quantity Wl/M_p which is determined for any particular mechanism by a virtual work analysis, and minimising W for given values of M_p and l amounts to maximising M_p for given values of W and l.

To summarise, then, the proposed method is as follows:

(1) Determine the correct number of independent mechanisms by calculating the number of independent equations of equilibrium.
(2) Calculate the required values of the fully plastic moments of the members by virtual work for these independent mechanisms.
(3) Investigate combinations of these mechanisms so as to maximise the required fully plastic moments.
(4) Check the solution by constructing a bending moment diagram.

An application of the method to a single-bay pitched-roof portal frame will now be given in detail, followed by a brief indication of the application of the method to a three-bay pitched-roof portal frame.

PITCHED-ROOF PORTAL DESIGN

As an illustration of the practical application of the proposed method of design, typical calculations for a pitched-roof portal frame will now be given. The dimensions of the frame are as indicated in fig. 5, the roof slope being $22\frac{1}{2}°$. The working loads on the frame are also shown in fig. 5. These working loads, which are given in tons, are assumed to be spread uniformly over the purlins and sheeting rails shown in the figure. Of these loads, the vertical loads of 2·61 tons, acting on each rafter, are due to dead and superimposed (snow) loads, and the remaining loads are wind pressures and suctions. The frame is to be designed to a load factor of 1·75 for the case in which only the dead and superimposed loads are acting, and to a load factor of 1·4 for the case in which the wind loads are also acting. Each member of the frame will be taken to have the same cross-section, with a fully plastic moment M_p.

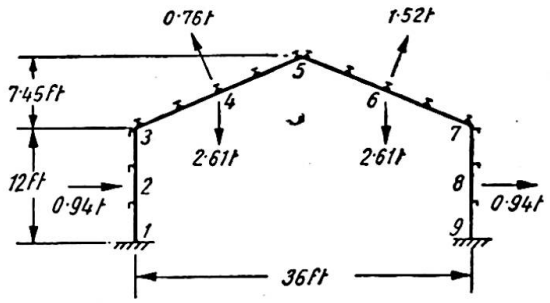

Fig. 5

Design for dead, superimposed and wind loads

The first design case which will be considered is the design to a load factor of 1·4 for the case in which the wind loads are acting in conjunction with the dead and superimposed loads. The first step is to decide how many independent partial collapse mechanisms must be considered. The number of such mechanisms for any given frame and loading has been shown to be equal to the number of independent equations of equilibrium. It is therefore necessary to calculate the number of independent equations of equilibrium, and this is done most conveniently by counting the number of bending moments which are needed to specify the bending moment distribution for the entire frame and subtracting the number of redundancies.

For each of the four members of the frame, the loads will be assumed to be uniformly distributed, so that the distribution of bending moment is parabolic. Each parabola will be completely specified if the values of the bending moment at three sections are known. These three sections are chosen most conveniently for the present purpose as the two end sections and the central section in each member. It follows that the bending moment distribution for the entire frame will be specified completely by the values of the bending moments at the nine cross-sections numbered

from 1 to 9 in fig. 5. This frame has three redundancies, and so there must be six independent equations of equilibrium.

It follows that there must be six independent partial collapse mechanisms. These mechanisms are illustrated in figs. 6–11, inclusive. It will be seen that the mechanisms of figs. 6, 7, 8 and 9 are merely simple beam failure mechanisms, and fig. 10 shows a simple sidesway mechanism. If it were not known that there must be six independent mechanisms, it might be concluded that these five mechanisms constituted the independent partial collapse mechanisms, and thus a calculation of the correct number of independent mechanisms is a vital preliminary operation in the analysis. However, a sixth independent mechanism must be selected, and the most convenient choice is the mechanism shown in fig. 11. In each figure the rotation of each plastic hinge is given in terms of a single variable θ. There is no need to consider the signs of the plastic hinge rotations, since the virtual work absorbed in a plastic hinge is always positive. However, for convenience in the later stages of the calculations when the solution is checked by statics, the signs of the plastic hinge rotations are also given, the sign convention being that a hinge rotation is positive if the joint is opening when viewed from within the portal.

In the simple beam failure mechanisms of figs. 6, 7, 8 and 9, the plastic hinges within the spans are all shown as occurring at mid-span. However, the loads on these spans are all assumed to be uniformly distributed in the first instance, so that these plastic hinges might occur anywhere within the spans. This is because a plastic hinge within a span must occur at a position of maximum bending moment, and the positions at which the maximum bending moments occur are not known until a later stage in the analysis. However, in the preliminary calculations it is convenient to take these plastic hinges as occurring in mid-span.

Now consider the mechanism of fig. 6. For the hinge rotations shown, the plastic hinge at mid-span moves through a distance 6θ ft. The average displacement of the uniformly distributed load of 0·94 tons is therefore 3θ ft., so that the virtual work done by this load, taking into account the load factor of 1·4, is $0{\cdot}94 \cdot 1{\cdot}4 \cdot 3\theta$ tons-ft. The total plastic hinge rotation involved in the mechanism is 4θ, so that the virtual work absorbed in the plastic hinges is $4\theta M_p$. Applying the principle of virtual work, it is found that

$$4\theta M_p = 0{\cdot}94 \cdot 1{\cdot}4 \cdot 3\theta = 3{\cdot}95\theta$$
$$M_p = 0{\cdot}99 \text{ tons-ft.} \quad \ldots\ldots\ldots\ldots \quad (7)$$

The virtual work equation for the mechanism of fig. 7 is precisely the same as

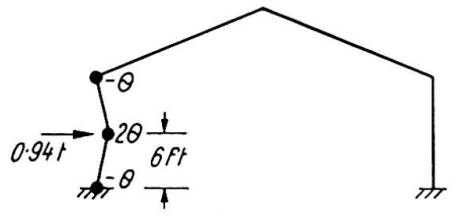

Fig. 6

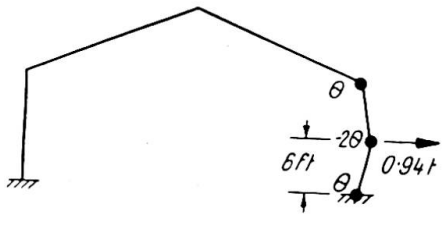

Fig. 7

equation (7). Corresponding virtual work equations may be written down at once for the mechanisms of figs. 8 and 9. These equations are:

fig. 8:
$$4\theta M_p = 1{\cdot}4[2{\cdot}61 \cdot 4{\cdot}5\theta - 0{\cdot}76 \cdot 4{\cdot}87\theta] = 11{\cdot}3\theta$$
$$M_p = 2{\cdot}83 \text{ tons-ft.} \quad \ldots\ldots\ldots\ldots \quad (8)$$

fig. 9:
$$4\theta M_p = 1{\cdot}4[2{\cdot}61 \cdot 4{\cdot}5\theta - 1{\cdot}52 \cdot 4{\cdot}87\theta] = 6{\cdot}08\theta$$
$$M_p = 1{\cdot}52 \text{ tons-ft.} \quad \ldots\ldots\ldots\ldots \quad (9)$$

The geometry of the sidesway mechanism of fig. 10 is also simple. Each side load of 0·94 tons moves through an average distance of 6θ ft., and the entire roof moves laterally through a distance 12θ ft. The virtual work equation is

$$4\theta M_p = 1{\cdot}4[2\,.\,0{\cdot}94\,.\,6\theta + 0{\cdot}76 \sin 22\tfrac{1}{2}^\circ\,.\,12\theta] = 20{\cdot}7\theta$$

$$M_p = 5{\cdot}18 \text{ tons-ft.} \quad . \quad . \quad . \quad . \quad . \quad . \quad . \quad . \quad . \quad . \quad . \quad . \quad (10)$$

The geometry of the mechanism of fig. 11 is a little more complicated. If the hinge at joint 3 rotated through an angle $-\theta$ while the joint 5 remained rigid, joint 7 would

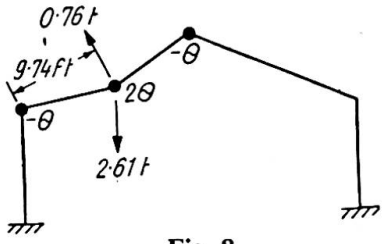

Fig. 8

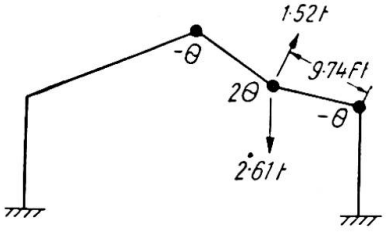

Fig. 9

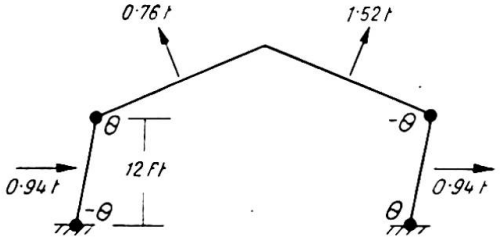

Fig. 10

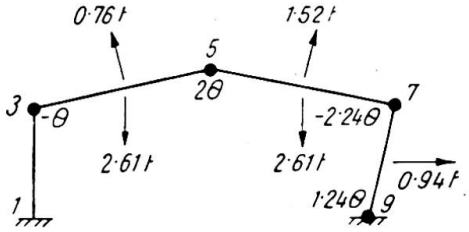

Fig. 11

move downwards through a distance 36θ ft. Since there can be no downwards motion of joint 7 for a small displacement of the mechanism, it follows that the hinge at joint 5 must rotate through an angle $36\theta/18 = 2\theta$ so as to reduce the vertical displacement of joint 7 to zero. This hinge rotation causes a horizontal displacement of joint 7 through a distance $2\theta\,.\,7{\cdot}45 = 14{\cdot}9\theta$ ft., so that the rotation of the hinge at joint 9 is $14{\cdot}9\theta/12 = 1{\cdot}24\theta$. The hinge rotation at joint 7 is then seen to be $-2{\cdot}24\theta$, and it is found that the centre of the member 57 moves $11{\cdot}2\theta$ ft. to the right and 9θ ft. downwards. The virtual work equation for this mechanism may now be written down as follows:

$$6{\cdot}48\theta M_p = 1{\cdot}4[2\,.\,2{\cdot}61\,.\,9\theta - 0{\cdot}76\,.\,9{\cdot}74\theta + 1{\cdot}52 \sin 22\tfrac{1}{2}^\circ\,.\,11{\cdot}2\theta$$
$$- 1{\cdot}52 \cos 22\tfrac{1}{2}^\circ\,.\,9\theta + 0{\cdot}94\,.\,7{\cdot}45\theta]$$
$$= 56{\cdot}6\theta$$
$$M_p = 8{\cdot}73 \text{ tons-ft.} \quad . \quad . \quad . \quad . \quad . \quad . \quad . \quad . \quad . \quad . \quad . \quad . \quad (11)$$

Among the six independent partial collapse mechanisms, the highest values of M_p are thus 5·18 tons-ft. and 8·73 tons-ft. for the mechanisms of figs. 10 and 11, respectively. The next step is thus to investigate the combination of these two mechanisms. It is seen that if the mechanism of fig. 10 is superposed on the mechanism of fig. 11, the rotation of the hinge at joint 3 is cancelled, so that the resulting mechanism is as shown in fig. 12. The virtual work equation for this mechanism is obtained by adding equations (10) and (11), and subtracting $2\theta M_p$ from the resulting virtual work

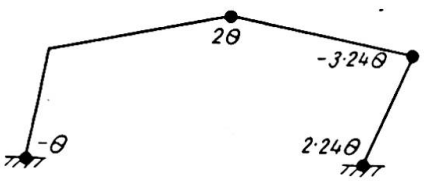

Fig. 12

absorbed in the plastic hinges, since a term θM_p was included in each of these equations for the plastic hinge at joint 3. The virtual work equation is thus:

$$(4+6\cdot48-2)\theta M_p=20\cdot7\theta+56\cdot6\theta$$

$$8\cdot48\theta M_p=77\cdot3\theta$$

$$M_p=9\cdot12 \text{ tons-ft.} \quad . \quad . \quad . \quad . \quad . \quad (12)$$

The highest value of M_p obtained from the other four independent mechanisms of figs. 6, 7, 8 and 9 was 2·83 tons-ft. for the mechanism of fig. 8, and it is readily seen that there is no possible combination of these mechanisms with the mechanism of fig. 12 which will result in a further increase in the value of M_p. It is therefore concluded that the mechanism of fig. 12 is the actual collapse mechanism, subject to the proviso that no consideration has yet been given to the possibility of the occurrence of plastic hinges at positions other than those numbered from 1 to 9 in fig. 5. When this solution is checked by statics it will, in fact, be found that the plastic hinge shown at the apex of the roof in fig. 12 should be located somewhat to the left of the apex.

Check by statics

The solution can be checked by constructing a bending moment diagram for the frame. If the fully plastic moment is not exceeded at any cross-section, the solution is correct. The actual bending moment at a cross-section may be regarded as the sum of the "free bending moment," produced in the frame by the applied loads when a cut has been made at some cross-section so as to render the frame statically determinate, and the "redundant bending moment" produced in the frame by the three redundancies. For convenience, the form of the redundant bending moment diagram will be considered first.

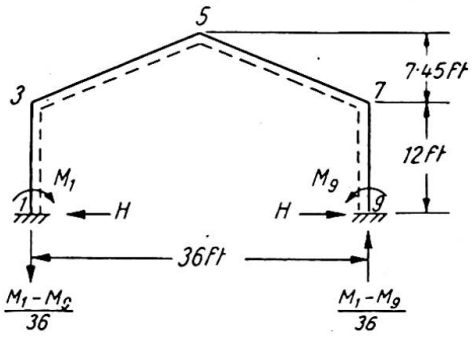

Fig. 13

The three redundancies may be taken as the bending moments, M_1 and M_9, at the feet of the vertical members, and the horizontal thrust H, as in fig. 13. With no external loads acting on the structure, the vertical reactions at the feet of the vertical members would be equal and opposite, and of magnitude $(M_1-M_9)/36$ as shown in the figure. In drawing the bending moment diagrams, the sign convention will be that a positive bending moment will cause a member to sag inwards, and thus to produce tension in the flange of the member which is adjacent to the dotted line in fig. 13. With the redundancies as shown in this figure, the redundant bending moment diagram is thus of the form indicated in fig. 14, in which the members of the frame have been redrawn to a horizontal base, and positive bending moments are plotted as ordinates below this base. In fig. 14 the dotted line

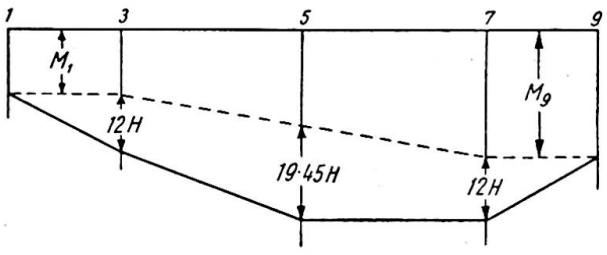

Fig. 14

indicates the form of the redundant bending moment diagram for the case in which H is zero, and the full line indicates the effect of superposing the bending moment diagram for the case in which H acts alone.

The free bending moment diagram refers to the bending moments produced in the frame by the applied loads when a cut is made at any arbitrary cross-section. The most convenient choice of cross-section for this purpose is the roof apex. Fig. 15 shows the free bending moment diagram, consisting of three parabolas, which is obtained in this way, the loads having been multiplied by the load factor of 1·4.

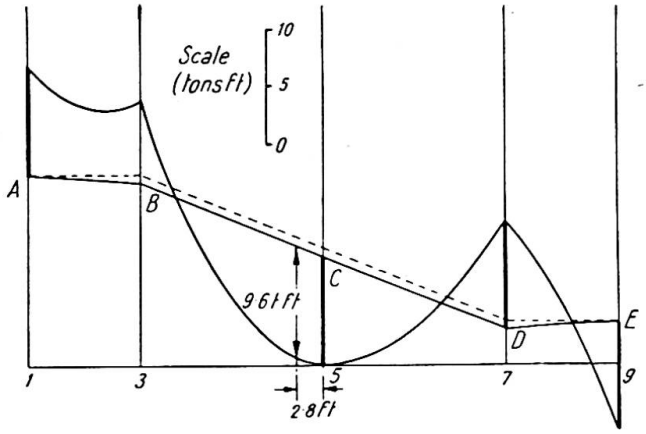

Fig. 15

The collapse mechanism of fig. 12 has four plastic hinges at the cross-sections 1, 5, 7 and 9, so that at these cross-sections the bending moment has its fully plastic value, which was found to be 9·1 tons-ft. To check the solution, it must be verified that a diagram of actual bending moments can be constructed in which the bending moment has the value 9·1 tons-ft. at these four cross-sections, and does not exceed this value at any other cross-section in the frame. Now the actual bending moment is equal to the sum of the free and redundant bending moments, so that if a redundant bending moment diagram is drawn in fig. 15 with the signs of the bending moments changed, the actual bending moment will be represented by the difference in ordinate between this diagram and the free bending moment diagram. The appropriate diagram is shown in fig. 15 as ABCDE.

The construction for this diagram is to lay off from the free bending moment diagram the calculated fully plastic moment of 9·1 tons-ft., with appropriate sign, at the four cross-sections 1, 5, 7 and 9. This gives the four points A, C, D and E on the redundant bending moment diagram. Referring to fig. 14, it is seen that the point B may then be plotted by making the slope of AB equal in magnitude to the slope of DE, but of opposite sign. A check can then be made by observing that the vertical intercept between C and the dotted line in fig. 15 is 19·45 H, whereas the corresponding intercept at D is 12 H. These intercepts both correspond to a value of H of 0·05 tons, thus checking the solution. However, it will be seen that although the bending moment at the cross-section 3 is less than the calculated fully plastic moment of 9·1 tons ft., a higher value of the bending moment occurs at a distance of 2·8 ft. along the left-hand rafter member from the apex joint, this value being 9·6 tons-ft. This does not imply an error in the virtual work calculations, for in those calculations the choice of plastic hinge positions was restricted to the ends and centres of the members. The calculation of the required fully plastic moment could be refined by carrying out

a fresh virtual work calculation in which the plastic hinge at the apex joint 5 was moved to the new position 2·8 ft. along the left-hand rafter member. However, it is unnecessary to perform this calculation, for it will be seen that the design is, in fact, not governed by this loading case but by the dead and superimposed loading case. It is therefore noted that a value of M_p between 9·1 and 9·6 tons-ft. would be adequate for dead, superimposed and wind loads in conjunction.

Design for dead and superimposed loads

The design for dead and superimposed loads to a load factor of 1·75 will now be considered. The relevant working loads are merely loads of 2·61 tons uniformly distributed over the two rafters, as shown in fig. 16. Since this loading is symmetrical, the bending moment distribution for the frame is also symmetrical, and so only four bending moments are needed to specify the bending moment distribution. These may be taken as the bending moments at the cross-sections 1, 3, 4 and 5 in fig. 16. Due to symmetry, the frame has only two redundancies, for the bending moments at the cross-sections 1 and 9 are equal. The bending moment at cross-section 1 and the horizontal thrust can thus be regarded as the two redundancies. It follows that there are only two equations of equilibrium, and therefore two independent mechanisms. Both of these mechanisms must be symmetrical.

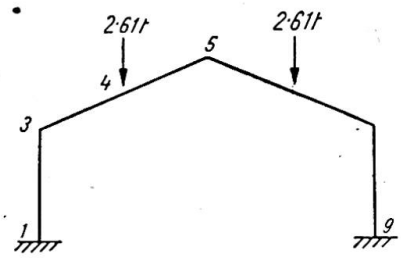

Fig. 16

The two independent mechanisms are illustrated in figs. 17 and 18. Fig. 17 merely represents failure of the two rafters as beamS, and the equation of virtual work is

$$8\theta M_p = 2 \,.\, 2{\cdot}61 \,.\, 1{\cdot}75 \,.\, 4{\cdot}5\theta = 41{\cdot}1\theta$$

$$M_p = 5{\cdot}14 \text{ tons-ft.} \quad . \quad . \quad . \quad . \quad . \quad . \quad . \quad . \quad . \quad . \quad . \quad (13)$$

In the mechanism of fig. 18, the hinge rotation θ at cross-section 1 would produce a horizontal movement of $19{\cdot}45\theta$ at the roof apex if there were no hinge rotation

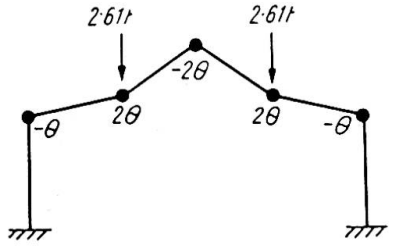

Fig. 17

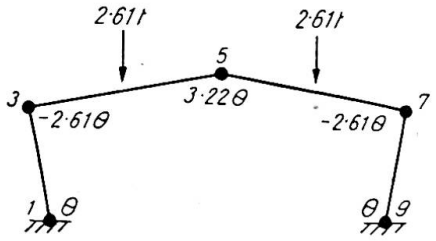

Fig. 18

at cross-section 3. The hinge rotation at cross-section 3 must therefore be $-19{\cdot}45\theta/7{\cdot}45 = -2{\cdot}61\theta$ in order that there should be no horizontal movement at the apex. The downwards vertical displacement at the apex is thus $18 \,.\, 1{\cdot}61\theta = 29{\cdot}0\theta$ ft. The virtual work equation is:

$$10{\cdot}44\theta M_p = 2 \,.\, 2{\cdot}61 \,.\, 1{\cdot}75 \,.\, 14{\cdot}5\theta = 132{\cdot}5\theta$$

$$M_p = 12{\cdot}7 \text{ tons-ft.} \quad . \quad . \quad . \quad . \quad . \quad . \quad . \quad . \quad . \quad . \quad . \quad (14)$$

It will be noted that this value of M_p exceeds the value found for the case in which the wind loads act in conjunction with the dead and superimposed loads. It follows

that the design must be governed by the present case in which only the dead and superimposed loads are acting.

Considering now the combination of the independent mechanisms, it will be seen that cancellation of the plastic hinge rotation at the roof apex can be achieved by superposing the mechanism of fig. 17, with all the hinge rotations and displacements increased by a factor of $3{\cdot}22/2=1{\cdot}61$, on the mechanism of fig. 18. The mechanism thus obtained is illustrated in fig. 19. The virtual work equation for this mechanism is obtained by adding equation (13), multiplied by 1·61, to equation (14), and subtracting $6{\cdot}44\theta M_p$ from the resulting virtual work absorbed in the plastic hinges, since a plastic hinge rotation of $3{\cdot}22\theta$ in each of the mechanisms at the roof apex has been cancelled. The resulting equation is:

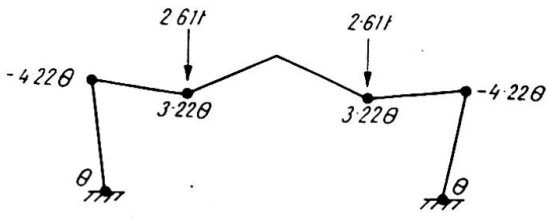

Fig. 19

$$(8\ .\ 1{\cdot}61+10{\cdot}44-6{\cdot}44)\ \theta M_p=41{\cdot}1\ .\ 1{\cdot}61\theta+132{\cdot}5\theta$$

$$16{\cdot}88\theta M_p=198{\cdot}7\theta$$

$$M_p=11{\cdot}8 \text{ tons-ft.} \quad . \quad . \quad . \quad . \quad . \quad . \quad (15)$$

The highest value of M_p obtained from these mechanisms is thus 12·7 tons-ft. for the mechanism of fig. 18. This is therefore the actual collapse mechanism, subject to possible alterations due to the occurrence of plastic hinges within the spans of the members rather than at the joints. A statical check will reveal, in fact, that the plastic hinge at the roof apex should be replaced by one plastic hinge in each rafter member.

Check by statics

The free bending moment diagram for the frame, cut at the roof apex, when subjected to the factored loads, is shown in fig. 20, together with the redundant bending moment diagram. This latter diagram is constructed by setting off the calculated fully plastic moment of 12·7 tons-ft. from the free bending moment diagram at the

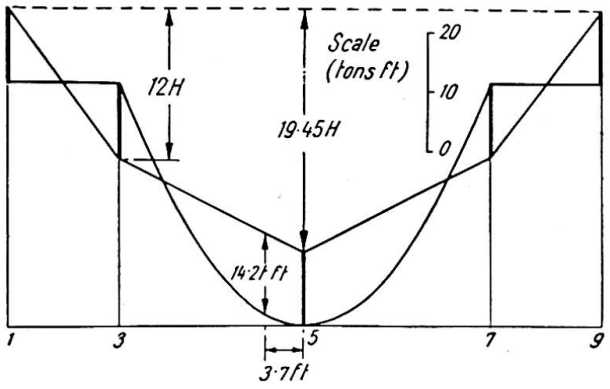

Fig. 20

cross-sections 1, 3, 5, 7 and 9. The value of the horizontal thrust can be calculated from the intercepts between the redundant bending moment line and the dotted line in fig. 20 at both the cross-sections 3 and 5. The value obtained in each case is 2·1 tons, thus checking the virtual work calculation. It will be seen that the greatest bending moment which occurs with this bending moment distribution is 14·2 tons-ft. at a distance of 3·7 ft. from the roof apex. Thus in the correct collapse mechanism

there should be plastic hinges in each rafter at a distance of about 3·7 ft. from the roof apex in place of the single plastic hinge shown at the apex in fig. 18. A fresh calculation for these new plastic hinge positions is readily made, either by virtual work or by adjusting the redundant bending moment line on the bending moment diagram, and the resulting value of M_p is found to be 13·2 tons-ft. A final refinement is to take account of the fact that the loads are not, in fact, uniformly distributed over the rafters, but are carried by five uniformly spaced purlins, as shown in fig. 5. The plastic hinges in the rafters will be located beneath the purlins which are adjacent to the roof apex, and the corresponding value of M_p is found to be 13·0 tons-ft. or 156 tons-in.

A choice of section can now be made. The fully plastic moment for a rolled steel joist is known to exceed the moment at which the yield stress is just reached in the outermost fibres by a factor termed the shape factor, which is about 1·15 for most sections.[4] Taking a yield stress of 15·25 tons/in.^{2}, the fully plastic moment M_p is thus:

$$M_p = 1{\cdot}15 \,.\, 15{\cdot}25 \,.\, Z = 17{\cdot}5\, Z \text{ tons-in.}$$

where Z in.^{3} is the section modulus. The required value of Z in the present case is:

$$Z = 156/17{\cdot}5 = 8{\cdot}91 \text{ in.}^3$$

The nearest available British Standard beam section is a 7×4×16 lb., with a section modulus of 11·29 in.^{3} This is therefore the required section. From the point of view of stability, the purlins and sheeting rails, together with some cross-bracing, would provide adequate stiffening for this section over the given spans.

THREE-BAY PITCHED-ROOF PORTAL FRAME

To illustrate the scope of the technique which has been described in detail, calculations for the three-bay frame whose dimensions and loads are as shown in fig. 21 will now be outlined briefly. As before, all the loads are assumed to be uniformly

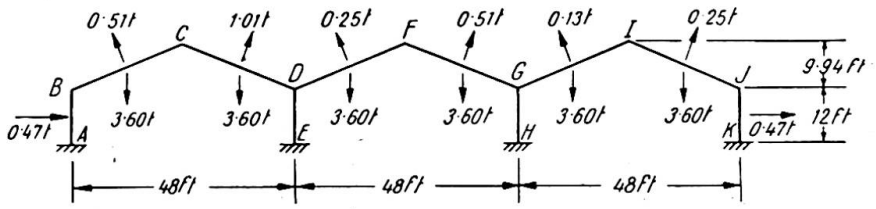

Fig. 21

distributed, and the vertical loads of 3·60 tons on each rafter member are due to dead and superimposed loads, the remaining loads being wind loads. In the first instance, it will be assumed that all the members of the frame are of the same cross-section, with a fully plastic moment M_p.

Design for dead, superimposed and wind loads

For this loading case, a load factor of 1·4 will be used. Examination of fig. 21 shows that twenty-three bending moments are needed to specify the bending moment distribution for the entire frame, which has nine redundancies. There must therefore be fourteen independent mechanisms. Eight of these mechanisms are accounted for by the simple beam type of failure mechanism (as in figs. 6, 7, 8 and 9, for example) occurring in the members AB, BC, CD, DF, FG, GI, IJ and JK. For these mechanisms, the highest value of M_p is obtained for the member GI, this value of M_p being

7·28 tons-ft. Two mechanisms must be counted for rotations of the joints D and G in fig. 21, for it will be realised that for each of these joints there will be an equation of rotational equilibrium between the three bending moments acting on the joint. There will also be one sidesway mechanism, with plastic hinges in the vertical members at A, B, D, E, G, H, J and K, for which the corresponding value of M_p is 1·69 tons-ft. The remaining three independent mechanisms may be chosen in a variety of ways, but the three mechanisms illustrated in figs. 22, 23 and 24 are probably the most convenient for the present purpose. It will be seen that each of these mechanisms is basically of the same type, with the rafters collapsing in one bay and thus causing sidesway of those parts of the frame lying to the right of the collapsing bay. For reference, the plastic hinge rotations are shown in these figures in magnitude only. It will be noted that the joints D and G remain unrotated in each of these mechanisms, since in each case any rotation of these joints would increase the work absorbed in the plastic hinges and so reduce the value of M_p.

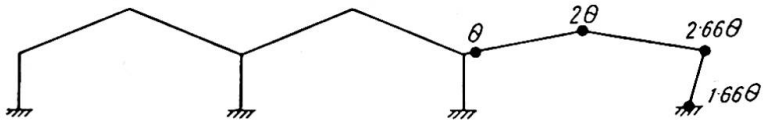

Fig. 22

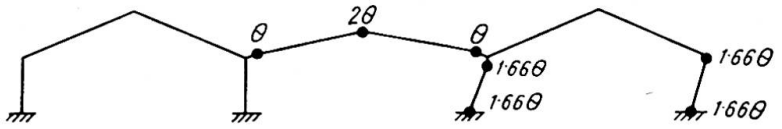

Fig. 23

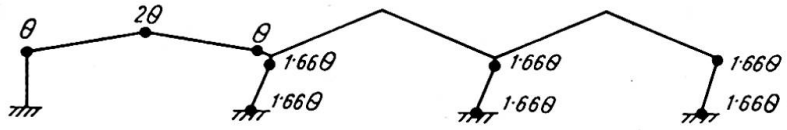

Fig. 24

The virtual work equations for these three mechanisms are found to be:

fig. 22: $7{\cdot}32\theta M_p = 123{\cdot}5\theta$, $M_p = 16{\cdot}9$ tons-ft. . . . . (16)

fig. 23: $10{\cdot}64\theta M_p = 120{\cdot}4\theta$, $M_p = 11{\cdot}3$ tons-ft. . . . . (17)

fig. 24: $13{\cdot}96\theta M_p = 115{\cdot}1\theta$, $M_p = 8{\cdot}25$ tons-ft. . . . . (18)

The highest value of M_p obtained from the independent mechanisms is thus 16·9 tons-ft. for the mechanism of fig. 22. It is easily seen that this value of M_p will not be increased by combination with any of the simple beam mechanisms, for which the highest value of M_p was found to be 7·28 tons-ft. It is also clear that the sidesway mechanism, for which M_p was found to be only 1·69 tons-ft., cannot be combined with advantage. It remains to investigate possible combinations of the three mechanisms of figs. 22, 23 and 24.

The mechanisms of figs. 22 and 23 can be combined if the hinge rotations and displacements in the mechanism of fig. 22 are all multiplied by a factor of 1·66, and

then superposed on the mechanism of fig. 23. This enables a clockwise rotation, of magnitude $1{\cdot}66\theta$, to be given to joint G, which cancels plastic hinge rotations of $1{\cdot}66\theta$ in the members GI and GH at this joint, while increasing the plastic hinge rotation in the member GF by $1{\cdot}66\theta$. This produces a net reduction in the virtual work absorbed of $1{\cdot}66\theta M_p$. The resulting virtual work equation for this combination is then seen from equations (16) and (17) to be:

$$1{\cdot}66 \,.\, 7{\cdot}32 \,.\, \theta M_p + 10{\cdot}64\theta M_p - 1{\cdot}66\theta M_p = 1{\cdot}66 \,.\, 123{\cdot}5\theta + 120{\cdot}4\theta$$

$$21{\cdot}1\theta M_p = 325\theta$$

$$M_p = 15{\cdot}4 \text{ tons-ft.} \quad . \quad . \quad . \quad . \quad (19)$$

This value of M_p is smaller than the value of 16·9 tons-ft. obtained for the mechanism of fig. 22, and it is clear that no other possible combination of the three mechanisms of figs. 22, 23 and 24 will yield a larger value of M_p. It is therefore concluded that the mechanism of fig. 22 is the actual collapse mechanism. This solution will not be adjusted to allow for the possible occurrence of plastic hinges at cross-sections other than the ends and centres of the members, for when the dead plus superimposed loading case is considered, it will be found that the wind loading case does not govern the design.

An interesting feature brought out by this analysis is that there are only four plastic hinges in the collapse mechanism, whereas the frame has nine redundancies. At collapse, therefore, only the right-hand bay of the frame is statically determinate, and in carrying out a statical check the bending moment diagram for the other two bays could not be constructed directly. Instead, it would be necessary to carry out a trial and error investigation to show that the six redundancies of these two bays could be chosen in at least one way so as to produce a resultant bending moment diagram in which the fully plastic moment was not exceeded anywhere in the frame. This would be a tedious process, and in view of the fact that this is not the loading case which governs the design, the check is probably not worth performing.

Design for dead and superimposed loads

A load factor of 1·75 will be used for this loading case. The loading, consisting merely of the vertical loads of 3·60 tons on each rafter, is symmetrical, so that the collapse mechanism and the bending moment distribution at collapse must also be symmetrical. It will be seen that the values of eleven bending moments will specify the bending moment distribution for the entire frame, and that owing to symmetry there are only five redundancies. There are thus six independent mechanisms, which must all be symmetrical. Three of these mechanisms are the simple beam type of failure mechanism in the *pairs* of rafters BC and IJ, CD and GI, and DF and FG. For each of these mechanisms, the corresponding value of M_p is 9·45 tons-ft. One mechanism must be counted for rotation of the joints D and G. The remaining two mechanisms are most conveniently chosen as the mechanisms shown in figs. 25 and 26.

The virtual work equations for these two mechanisms are:

fig. 25: $14{\cdot}64\theta M_p = 302{\cdot}4\theta, \quad M_p = 20{\cdot}6$ tons-ft. . . . . (20)

fig. 26: $10{\cdot}64\theta M_p = 151{\cdot}2\theta, \quad M_p = 14{\cdot}2$ tons-ft. . . . . (21)

The only possible combination of these mechanisms is obtained if the hinge rotations and displacements in the mechanism of fig. 25 are all multiplied by a factor of 0·83, and then superposed on the mechanism of fig. 26. This enables a counter-clockwise rotation of the joint D, of magnitude $0{\cdot}83\theta$, to be made, thus cancelling plastic rotations of $0{\cdot}83\theta$ in the members DC and DE at this joint, while increasing

the plastic hinge rotation in the member DF by $0{\cdot}83\theta$. This produces a net reduction in the virtual work absorbed of $0{\cdot}83\theta M_p$, and a similar reduction can be achieved by a clockwise rotation of the joint G. The resulting virtual work equation is then seen from equations (20) and (21) to be:

$$0{\cdot}83\,.\,14{\cdot}64\theta M_p+10{\cdot}64\theta M_p-1{\cdot}66\theta M_p=0{\cdot}83\,.\,302{\cdot}4\theta+151{\cdot}2\theta$$

$$21{\cdot}1\theta M_p=402\theta$$

$$M_p=19{\cdot}1 \text{ tons-ft.} \quad . \quad . \quad . \quad . \quad (22)$$

This value of M_p is less than the value of 20·6 tons ft. which was found to correspond to the mechanism of fig. 25. It may also be checked that the beam collapse mechanisms for the rafters cannot be combined with any of these mechanisms to produce a value

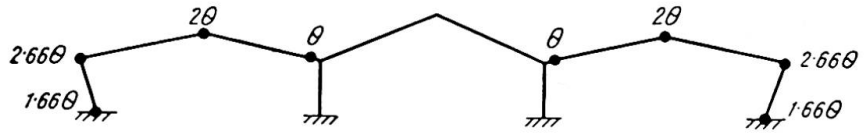

Fig. 25

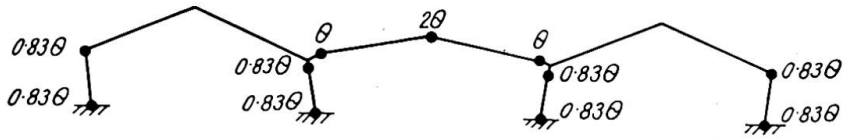

Fig. 26

of M_p greater than 20·6 tons-ft. The mechanism of fig. 25 is thus the actual collapse mechanism, subject to alterations due to the occurrence of plastic hinges at positions other than at the ends and centres of the members. A statical check will now be made which will also serve to indicate such alterations in the position of the plastic hinges.

Check by statics

Because of symmetry, the statical check need only be made for one half of the frame, say the left-hand half. For this portion of the frame, the free bending moment diagram is constructed by imagining cuts to be made at the apices C and F. The resulting diagram is given in fig. 27, for the case in which the loads have been multiplied by the load factor of 1·75. It will be seen that there is no free bending moment in the vertical member DE, and the diagram for this member has not been drawn.

For the members AB, BC and CD the redundant bending moment diagram may be constructed directly, since the bending moment has its fully plastic value at A, B, C and D. The horizontal thrust H in this bay can be calculated from the vertical intercept between the redundant bending moment diagram and the dotted line in fig. 27. In each case a value of 3·44 tons is obtained, thus checking the solution. Since the centre bay of the frame is not statically determinate at collapse, the redundant bending moment diagram for the member DF cannot be constructed directly. However, it is clear from the symmetry of the diagram about D that one possible redundant bending moment line for DF is the dotted line df shown in fig. 27, where fF represents the calculated fully plastic moment of 20·6 tons-ft. This line has a slope equal in magnitude to the line cd in fig. 27, and this corresponds to the same value of the

horizontal thrust of 3·44 tons which was found for the left-hand bay of the frame. If this were the actual redundant moment line for the member DF at collapse, it follows that there would be no resultant horizontal thrust on the vertical member DE, which would thus have zero bending moment throughout its length. It is therefore possible to construct a bending moment diagram for the entire frame in which the fully plastic moment is not exceeded at any cross-section, except within the spans of

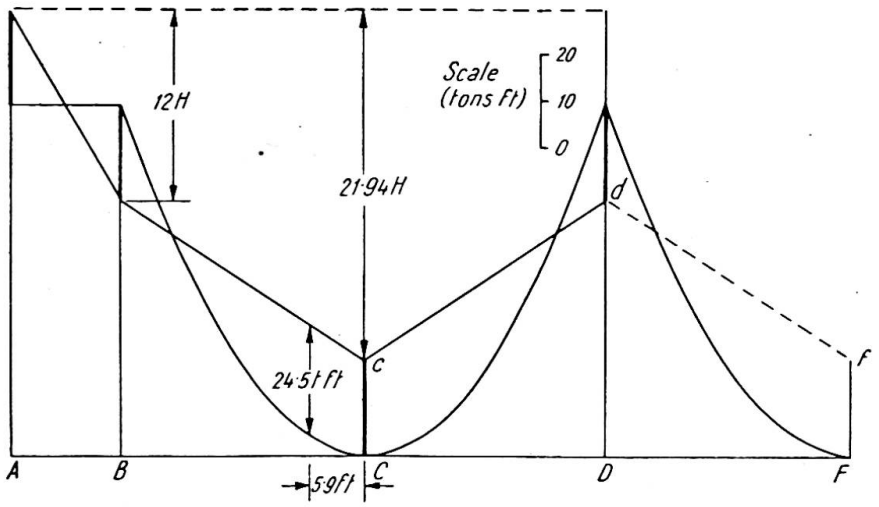

Fig. 27

the rafter members. This confirms that the correct solution was found by the virtual work analysis.

It will be seen from fig. 27 that plastic hinges will actually occur in the rafter members at distances of 5·9 ft. from the apices C and G, rather than at these apices. When this is taken into account, the value of M_p is found to be 21·9 tons-ft.

The statical check reveals the fact that the internal stanchions DE and GH need not be called upon to participate in the collapse mechanism, for it is possible to construct a resultant bending moment diagram in which these members are free from bending moment. These members, which were assumed in the first instance to possess a fully plastic moment M_p, thus function merely as props which hold up the rafter members. They could therefore be designed simply as compression members, and made of hollow tubing.

Conclusions

The merits of the method of design described in this paper can really be appreciated only by applying the method to practical examples. However, the foregoing examples serve to illustrate some of its advantages. The outstanding feature of the method is, of course, its rapidity. This is mainly due to the ease with which corresponding values of M_p can be obtained by the principle of virtual work, and this in turn is due largely to the fact that there is no need to establish sign conventions when applying this principle, since the virtual work absorbed in a plastic hinge must always be positive. A further important advantage of the method is that it enables solutions to be found without difficulty for those cases in which the entire frame is not statically determinate at collapse. Such cases have hitherto been somewhat intractable.

REFERENCES

(1) BAKER, J. F., "A Review of Recent Investigation into the Behaviour of Steel Frames in the Plastic Range," *J. Inst. Civ. Engrs.*, **31**, 188, 1949.
(2) BAKER, J. F., and HEYMAN, J, "Tests on Miniature Portal Frames," *The Structural Engineer*, **28**, 139, 1950.
(3) MAIER-LEIBNITZ, H. "Die Bedeutung der Zähigkeit des Stahles," *Prelim. Publ. 2nd Congress Intl. Assoc. Bridge and Structural Eng. Berlin*, 1936, p. 103.
(4) BAKER, J. F., "The Design of Steel Frames," *The Structural Engineer*, **27**, 397, 1949.
(5) NEAL, B. G., and SYMONDS, P. S., "The Calculation of Collapse Loads for Framed Structures," *J. Inst. Civ. Engrs.*, **35**, 20, 1950.
(6) GREENBERG, H. J., and PRAGER, W., "On Limit Design of Beams and Frames," *Proc. A.S.C.E.* **77**, *Separate* No. 59, 1951.
(7) NEAL, B. G., and SYMONDS, P. S., "The Rapid Calculation of the Plastic Collapse Load for a Framed Structure" (to be published in *Proc. Inst. Civ. Engrs. Part III*, **1**).
(8) HORNE, M. R., "Fundamental Propositions in the Plastic Theory of Structures," *J. Inst. Civ. Engrs.*, **34**, 174, 1950.

Summary

In suitable instances the application of plastic design methods to plane frames of ductile material, such as mild steel, leads to more rational and economical designs. These design methods are based on the calculation of the loads at which a structure collapses owing to excessive plastic deformation. Such collapses occur when a sufficient number of plastic hinges have formed to transform the structure into a mechanism, so that deflections can continue to grow, due to rotations of the plastic hinges, while the loads remain constant.

It is known that among all possible collapse mechanisms for a given frame and loading, the actual collapse mechanism is the one to which there corresponds the smallest possible value of the load. Recently, it has been pointed out that all the possible collapse mechanisms for a frame can be regarded as built up from a certain number of simple mechanisms. This has led to the development of a new technique for determining plastic collapse loads, in which these simple mechanisms are combined in a systematic manner so as to reduce the corresponding value of the load to its least possible value. For each mechanism which is investigated, the corresponding value of the load is determined very quickly by applying the Principle of Virtual Work.

In the present paper, the theoretical basis of this new technique is discussed, and typical calculations for a pitched-roof portal frame are given.

Résumé

Dans différents cas, l'application de la théorie de la plasticité au calcul des cadres plans en matériaux forgeables, comme l'acier fondu, conduit à des solutions rationnelles économiques. Cette méthode de calcul repose sur la détermination des charges sous lesquelles un ouvrage cède à la suite de déformations plastiques infiniment grandes. La rupture se produit à la suite de la formation d'articulations plastiques en nombre suffisant pour transformer l'élément porteur en un "mécanisme"; à la suite du processus de rotation des articulations plastiques, les déformations prennent des amplitudes de plus en plus grandes, tandis que la charge reste constante.

On sait que parmi tous les processus possibles de rupture d'un cadre donné sous l'action de conditions de mise en charge données, le processus décisif est celui qui correspond à la plus petite valeur possible de la charge. On a montré récemment que tous les processus possibles de rupture d'un cadre peuvent être considérés comme composés d'un certain nombre de processus habituels. Ceci a conduit à la mise au

point d'un nouveau procédé pour la détermination de la charge plastique de rupture, procédé dans lequel les processus simples sont combinés d'une manière systématique en vue de réduire la charge correspondante à sa plus petite valeur possible. Les valeurs de la charge peuvent être déterminées très rapidement pour chaque processus ainsi introduit, par l'application du principe des travaux virtuels.

Les auteurs discutent dans le présent rapport les bases théoriques du nouveau procédé et exposent les modes de calcul caractéristiques pour un cadre-portique avec toit incliné.

Zusammenfassung

In verschiedenen Fällen führt die Anwendung der Plastizitätstheorie bei der Berechnung ebener Rahmen aus schmiedbarem Material, wie z.B. Flusstahl, zu rationellen und wirtschaftlichen Lösungen. Diese Berechnungsmethode beruht auf der Bestimmung derjenigen Lasten, unter welchen ein Bauwerk infolge unendlich grossen plastischen Verformungen versagt. Das Versagen tritt ein, wenn sich plastische Gelenke in genügender Zahl ausgebildet haben, um das Tragwerk in einen Mechanismus umzuwandeln; als Folge der Drehungen der plastischen Gelenke vergrössern sich dann die Formänderungen weiter, während die Belastung konstant bleibt.

Es ist bekannt, dass unter allen möglichen Bruchmechanismen eines gegebenen Rahmens mit gegebener Belastungsanordnung derjenige massgebend ist, dem der kleinstmögliche Wert der Belastung entspricht. Unlängst wurde gezeigt, dass alle möglichen Bruchmechanismen eines Rahmens als aus einer gewissen Zahl von gewöhnlichen Mechanismen zusammengesetzt betrachtet werden können. Dies hat zur Entwicklung eines neuen Verfahrens zur Bestimmung der plastischen Bruchlast geführt, bei welchem die einfachen Mechanismen systematisch kombiniert werden, um so den entsprechenden Wert der Last zu seiner kleinstmöglichen Grösse zu reduzieren. Die Werte der Last können für jeden eingeführten Mechanismus sehr schnell durch Anwendung des Prinzips der virtuellen Arbeit bestimmt werden.

Im vorliegenden Aufsatz wird die theoretische Grundlage des neuen Verfahrens diskutiert, und es werden die typischen Berechnungen für einen Portalrahmen mit geneigtem Dach gegeben.